Seed-Mediated Synthesis of Gold Octahedra in High Purity and with Well-Controlled Sizes and Optical Properties

ARTICLE *in* CHEMISTRY - A EUROPEAN JOURNAL · APRIL 2011

Impact Factor: 5.73 · DOI: 10.1002/chem.201100365 · Source: PubMed

7 AUTHORS, INCLUDING:

Do Youb Kim
Korea Research Institute of Chemical Tech…
43 PUBLICATIONS **704** CITATIONS
SEE PROFILE

Taekyung Yu
Kyung Hee University
55 PUBLICATIONS **3,500** CITATIONS
SEE PROFILE

DOI: 10.1002/chem.201100365

VIP

Seed-Mediated Synthesis of Gold Octahedra in High Purity and with Well-Controlled Sizes and Optical Properties

Do Youb Kim,[a, b] Weiyang Li,[a] Yanyun Ma,[a] Taekyung Yu,[a] Zhi-Yuan Li,[c] O Ok Park,[b] and Younan Xia*[a]

Abstract: We report a facile method for the synthesis of uniform Au octahedra with well-controlled sizes and optical properties by seed-mediated growth. Starting from single-crystal seeds of Au spheres with a uniform size, we could reproducibly obtain Au octahedra with a narrow size distribution (<7% in standard deviation) and in high purity (>90%). Moreover, the edge lengths of these Au octahedra could be readily tuned in a controllable fashion from 16 to 77 nm by varying the amount of seeds, the concentration of $HAuCl_4$, or both. We have also investigated the effects of water and poly(vinyl pyrrolidone) (PVP) in the system, as well as the reaction temperature, on the evolution of octahedral shape.

Keywords: gold · growth mechanism · nanocrystals · octahedra · seeded growth · size control

Introduction

Gold nanocrystals have received considerable attention for many decades due to their remarkable properties, such as bio-inertness, versatility and reproducibility for surface modification, tunable localized surface plasmon resonance (LSPR), as well as unusual catalytic activity.[1–4] These unique properties have enabled many interesting and important applications in electronics, photonics, catalysis, and especially in biomedicine, with notable examples including imaging, drug delivery, DNA analysis, immunoassay, as well as cancer diagnosis and treatment.[4–10] Driven by these spectacular applications, there has always been a strong motivation to generate Au nanocrystals with controllable sizes and shapes.[11–13]

Thanks to the efforts from many groups, a myriad of methods including seed-mediated growth, template-directed growth, and ordinary solution-phase syntheses based on chemical, electrochemical, or photochemical reduction, have been developed for the syntheses of Au nanocrystals with different sizes and shapes.[14–19] Among these approaches, seed-mediated growth has attracted particular attention owing to its many advantages over other synthetic methods: including, for example, the operation can be separated into two steps—preparation of seeds and subsequent growth—to offer greater flexibility in controlling both the sizes and shapes of resultant nanocrystals;[20,21] the size distribution of resultant nanocrystals can often be improved through a "self-focusing" mechanism;[22,23] the crystallinity and morphology of resultant nanocrystals can be conveniently controlled by using different types of seeds (single crystal vs. multiple-twinned);[24] and it typically requires milder reaction conditions than a self-nucleation process, especially the reaction temperature.[25]

There are a number of methods now available for generating Au nanocrystals having an octahedral shape and tunable edge lengths.[26–33] For example, Cho et al. have demonstrated the synthesis of Au octahedra with edge lengths of 30, 50, and 60 nm by heating $AuCl_3$ in a mixture of poly(ethylene glycol) 600 (PEG 600) and poly(vinyl pyrrolidone) (PVP) at 125 °C for 6–48 h.[26] They have also modified the method to produce Au octahedra with edge lengths over a broader range from 20 to 320 nm by introducing HCl or NaOH into ethylene glycol in the presence of poly(diallyldimethylammonium) chloride (PDDA) at 195 °C.[27] Huang et al. prepared Au octahedra with sizes ranging from 30 to 150 nm using a hydrothermal approach at 110 °C.[28] Recently, Niu et al. reported the synthesis of Au octahedra with an edge length of 60 nm by seed-mediated growth in the presence of cetylpyridinium chloride (CPC).[29] Due to the use of Au seeds with a size of approximately 41 nm, their demonstration was limited to the synthesis of Au octahedra larger than 50 nm in edge length. Although these prior methods could be used to prepare uniform Au octahedra with certain sizes and in relatively high purity, there is still room for the development of a protocol that can generate Au octahedra

[a] D. Y. Kim, W. Li, Y. Ma, T. Yu, Prof. Y. Xia
Department of Biomedical Engineering
Washington University
Saint Louis, MO 63130 (USA)
E-mail: xia@biomed.wustl.edu

[b] D. Y. Kim, Prof. O. O. Park
Department of Chemical and Biomolecular Engineering
Korea Advanced Institute of Science and Technology
335 Gwahangno, Yuseong-gu, Daejeon 305-701 (Korea)

[c] Prof. Z.-Y. Li
Institute of Physics, Chinese Academy of Science
Beijing, 100080 (P. R. China)

Supporting information for this article is available on the WWW under http://dx.doi.org/10.1002/chem.201100365.

with well-controlled edge lengths and under mild experimental conditions. The uniformity in both size and shape also need to be greatly improved for Au octahedra below 50 nm in edge length. It is worth pointing out that the smallest Au octahedra that have been reported in literature were approximately 20 nm in edge length and the sample was characterized by a broad size distribution and poor purity.[27,31] Here we report the synthesis of Au octahedra with well-controlled sizes in the range of 16–77 nm, narrow size distributions (standard deviations $<7\%$), and in high purity ($>90\%$ for the as-obtained samples). The synthesis is based on the use of seeds that had a single-crystal structure, together with a spherical shape and uniform size. The sizes of the Au octahedra could be easily tuned in a controllable fashion by varying the amount of seeds, the concentration of $HAuCl_4$, or both.

Results and Discussion

The synthesis of Au octahedra involves two steps. In the first step, single-crystal seeds of Au spheres with a uniform size of approximately 11 nm were prepared by modifying a protocol reported by other groups.[34,35] Briefly, Au nanocrystallites of approximately 3 nm in size were prepared in water by the reduction of $HAuCl_4$ with $NaBH_4$ in the presence of cetyltrimethylammonium bromide (CTAB). Then, these nanocrystallites were allowed to grow into Au nanospheres with a larger and more uniform size in the presence of additional $HAuCl_4$, ascorbic acid (AA), and cetyltrimethylammonium chloride (CTAC). Figure S1A in the Supporting Information shows a typical transmission electron microscopy (TEM) image of an as-prepared sample of Au nanospheres that were uniform in both size ((11.4 ± 1.2) nm in diameter) and shape. It is worth pointing out that such uniform Au nanospheres could be routinely synthesized in high purity ($>98\%$) without involving any additional purification/separation process. Figure S1B shows a high-resolution TEM image (HRTEM) taken from an individual Au nanosphere, indicating that it was a single-crystal cuboctahedron (or truncated octahedron) with a rounded profile and enclosed by a mix of {100} and {111} facets on the surface.

In the second step, the 11 nm Au nanospheres served as seeds to grow Au nanocrystals with an octahedral shape. For a standard synthesis, 0.1 mL of the as-prepared suspension of seeds (3.7×10^{15} particles per L) was added to a mixture of *N,N*-dimethylformamide (DMF) (5.8 mL) and water (0.1 mL) that also contained $HAuCl_4$ (0.162 mM) and PVP (213 mM, in terms of repeating unit) at room temperature, and then capped and heated in an oil bath at 80 °C for 1 h. Figure 1A and B show typical scanning electron microscopy (SEM) and TEM images of the as-prepared Au octahedra, which had an edge length of (24.5 ± 1.6) nm and could be obtained in high purity ($>94\%$) without involving any additional purification. The HRTEM image (Figure 1C) taken from an individual Au octahedron shows a continuous fringe pattern with spacing of 0.235, 0.204, and 0.144 nm, which

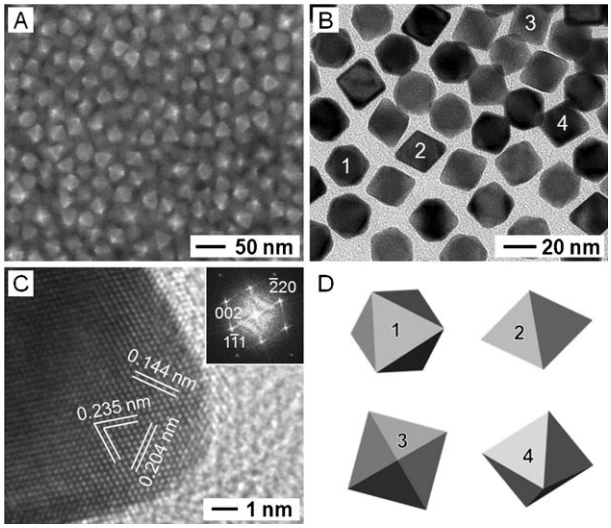

Figure 1. A) SEM and B) TEM images of the Au octahedra that were prepared using the standard procedure. C) HRTEM image taken from the corner region of a Au octahedron and the corresponding FFT pattern (inset). D) Schematics of an octahedron in four common orientations that correspond to the different, projected shapes of octahedron marked with the same numbers in (B).

could be indexed to the {111}, {200}, and {220} reflections of face-centered cubic (*fcc*) Au. The corresponding fast Fourier transform (FFT) pattern (inset in Figure 1C) confirms the single-crystal nature of the particle, indicating that this particle was sitting on the TEM grid along the [110] zone axis.[32,33] Figure 1D shows schematics of an octahedron in four common orientations that correspond to the different, projected shapes of octahedra marked with the same numbers in Figure 1B.

As a major advantage of a seed-mediated synthesis, the size of the Au octahedra could be readily controlled from approximately 16 nm to approximately 77 nm in edge length by simply varying the amount of seeds, the concentration of $HAuCl_4$, or both. Figure 2 shows TEM images of Au octahedra with different sizes obtained by adding different amounts of the as-prepared Au seeds into a set of reaction solutions containing the same amount of $HAuCl_4$. It can be seen that the edge lengths of the resultant Au octahedra increased from 16.2 to 22.3, 24.5, 27.8, 33.9, and 76.8 nm when the volume of the Au seed solution (3.7×10^{15} particles per L) was reduced from 150 to 120, 100, 70, 50, and 30 μL. It should be pointed out that the octahedra shown in Figure 2A exhibited a more or less spherical profile due to truncation at the corners (see the inset of Figure 2A). According to our calculation based on an ideal model of octahedron with a spherical seed in the center (see Figure S2 in the Supporting Information), the smallest octahedron that could be grown from a spherical seed of 11.4 nm in diameter was approximately 14 nm in edge length. In our experiments, the smallest Au octahedra we could obtain were approximately 16 nm in edge length. The difference between the experimental (16 nm) and theoretical values (14 nm)

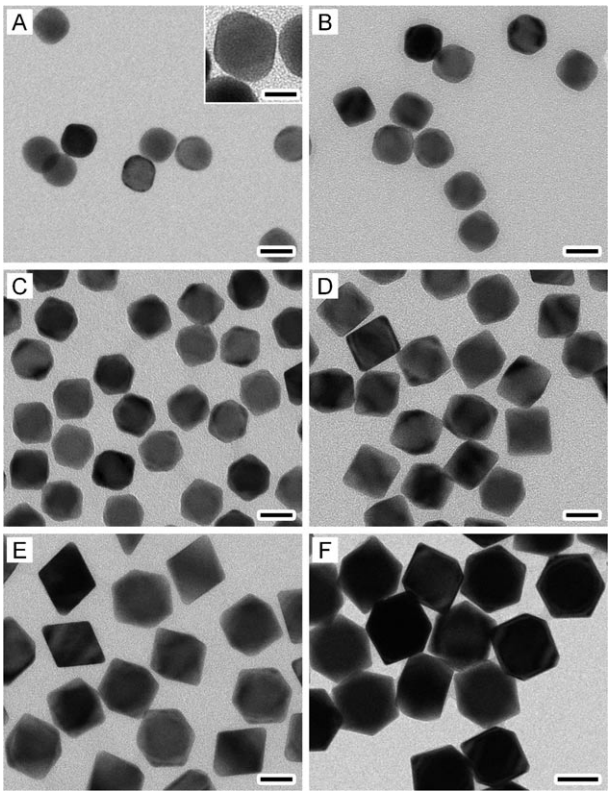

Figure 2. TEM images of Au octahedra with different edge lengths that were prepared using the standard procedure except different volumes (in parenthesis) of the Au seed suspension: A) 16.2 nm (150 μL), B) 22.3 nm (120 μL), C) 24.5 nm (100 μL), D) 27.8 nm (70 μL), E) 33.9 nm (50 μL), and F) 76.8 nm (30 μL), respectively. The inset in A shows a TEM image of the same sample at a higher magnification. The scale bars in A–E are 20 nm, and the scale bar in F is 50 nm. The scale bar in the inset is 10 nm.

could be attributed to the fact that the growth was not strictly limited to the <111> directions of a spherical seed.

The size of resultant octahedra could also be conveniently controlled by using $HAuCl_4$ solutions with different concentrations while the amount of seeds was kept the same. Figure 3A shows the TEM image of Au octahedra with an edge length of 17.3 nm that were prepared by using the standard procedure, except that the concentration of $HAuCl_4$ was reduced from 0.162 mM to 0.065 mM. When the concentration of $HAuCl_4$ was increased to 0.324 mM, Au octahedra with an edge length of 45.2 nm were obtained (Figure 3B). In this approach, the Au octahedra were also of good uniformity in terms of both size and shape. Table 1 summarizes

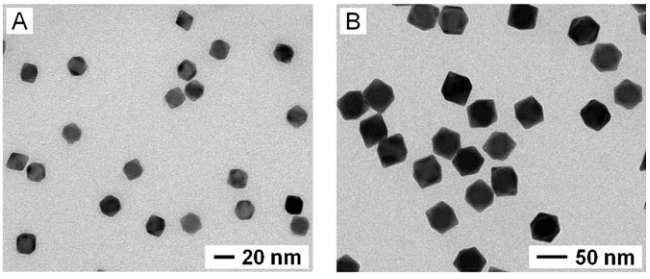

Figure 3. TEM images of Au octahedra with different edge lengths that were prepared using the standard procedure except the use of $HAuCl_4$ at two other different concentrations (in parenthesis): A) 17.3 nm (0.065 mM) and B) 45.2 nm (0.324 mM), respectively.

Table 1. Average edge length (L_{av}), standard deviation (σ), and percentage of Au octahedra obtained by using different amounts of seeds, or different concentrations of $HAuCl_4$ solution.

Seed solution[a] [μL]	L_{av} [nm]	σ [%]	Percentage of octahedra [%]
150	16.2	5.8	90
120	22.3	6.6	90
100	24.5	6.5	94
70	27.8	6.9	93
50	33.9	6.7	93
30	76.8	6.6	85
$HAuCl_4$[b] [mM]	L_{av} [nm]	σ [%]	Percentage of octahedra [%]
0.065	17.3	5.8	92
0.324	45.2	6.5	94

[a] The concentration of $HAuCl_4$ was 0.162 mM. [b] The volume of the Au seed suspension was 100 μL.

the average edge length, the standard deviation, and the percentage of Au octahedra in the as-prepared product. We can conclude that Au octahedra with a broad range of sizes (16–77 nm in edge length) could be routinely prepared with narrow size distributions and in high purity (>90% for the as-prepared samples). By reducing the size of Au seeds, it should also be possible to generate Au octahedra with sizes less than 16 nm.

The availability of uniform Au octahedra with a broad range of sizes allowed us to fully investigate the dependence of their LSPR properties on size. Figure 4A shows typical UV/Vis extinction spectra of the 11 nm spherical seeds and Au octahedra with different edge lengths. The spherical seeds had an LSPR peak at 520 nm. As the edge lengths of the Au octahedra gradually increased from 16.2 to 22.3, 27.8, 33.9, 45.2, and 76.8 nm, their LSPR peaks were red-shifted from 525 to 540, 553, 557, 564, and 599 nm, respectively. All peaks were very sharp, which can be attributed to the uniform size and shape of the Au octahedra. Figure 4B shows a plot of the LSPR peak position as a function of the edge length of Au octahedra. Obviously, the LSPR peak of the octahedron was red-shifted with increasing edge length, but we could not fit the correlation with a straight line. According to the extinction spectra theoretically calculated for Au octahedra, the LSPR peak position of a Au octahedron is not only dependent on its size but also the degree of truncation at corners (see Figure S3 in the Supporting Information). The calculations reveal that the LSPR peak position is clearly not linearly proportional to the edge length of an octahedron (in the range of 16–77 nm, with/without truncation at corners), and the LSPR peak of an octahedron is blue-shifted as the degree of truncation is increased. Table S1

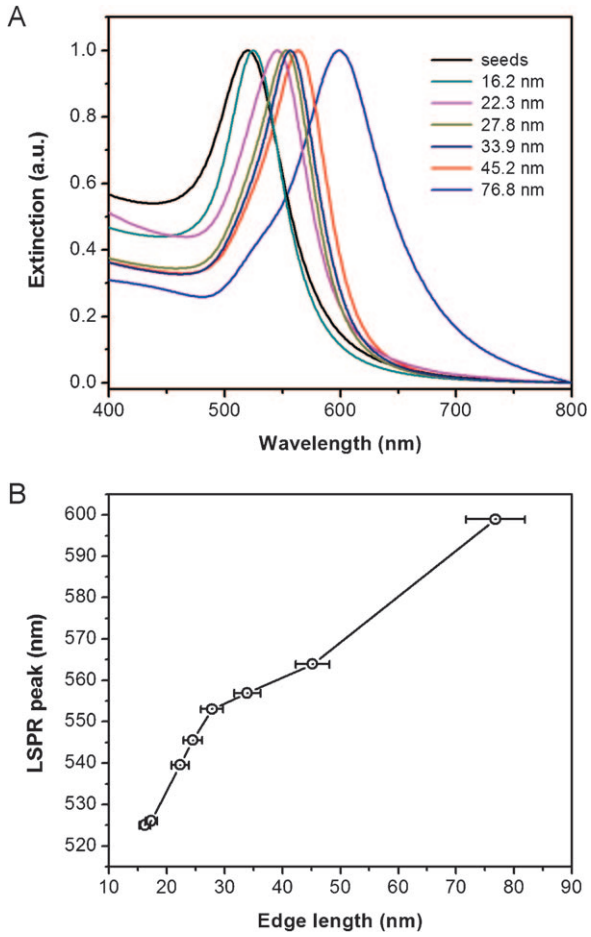

Figure 4. A) UV/Vis extinction spectra of the spherical Au seeds and Au octahedra with different edge lengths. B) Plot of the LSPR peak position as a function of the edge length of Au octahedra.

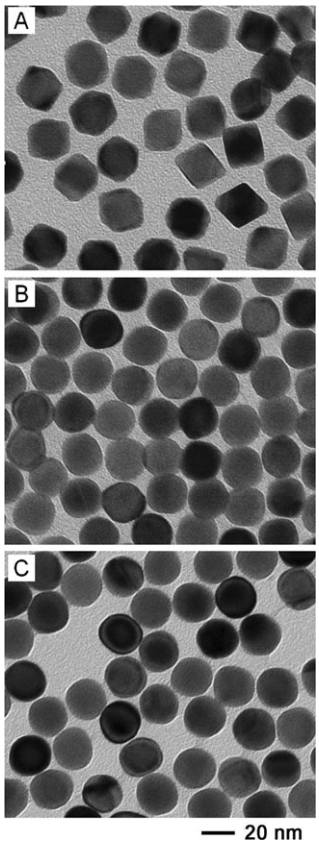

Figure 5. TEM images of Au nanocrystals prepared using the standard procedure except the addition of different amounts of water A) 0.1 mL, B) 0.6 mL, and C) 1.1 mL, respectively.

summarizes the LSPR peak positions of the as-obtained Au octahedra, as well as the Au octahedra with 0%, 10%, and 15% truncation at all corners simulated by calculations. We can see that the LSPR peaks for the as-obtained Au octahedra in all samples were considerably blue-shifted compared to the theoretically calculated values for those with perfect corners. When the edge length of the Au octahedra was relatively large (77 nm) and with a low degree of truncation (Figure 2F), the LSPR peak position was close to the value calculated for those with 10% truncation at corners. On the other hand, the LSPR peak positions for Au octahedra with edge lengths in a range from 28 to 45 nm were close to the values calculated for those with 15% truncation at corners. Furthermore, the LSPR peak positions for Au octahedra with relatively small edge lengths (16–22 nm) were even blue-shifted relative to the values calculated for those with 15% truncation, implying a degree of truncation >15% at corners for the as-obtained samples.

We further investigated the influence of water on the evolution of Au nanocrystals with an octahedral shape. Figure 5 shows TEM images of the Au nanocrystals prepared by using the standard procedure except the addition of different amounts of water to the reaction solution. When relatively small amounts of water (0.1 mL or 0.2 mL) were introduced into the reaction solution, the resultant Au nanocrystals exhibited an octahedral shape with sharp edges and corners, as shown in both Figure 1 and Figure 5A. As the amount of water in the reaction solution was increased to 0.6 mL, the as-obtained Au nanocrystals showed a more or less spherical profile (Figure 5B), which can be described as octahedra with significant truncation at the corners. When the amount of water was further increased to 1.1 mL, the as-obtained Au nanocrystals became essentially spherical (Figure 5C), indicating more significant truncation at the corners and edges. In our experimental system, the Au nanocrystals were generated by reducing $HAuCl_4$ with DMF in the presence of water, and the reaction can be described as the following:[36]

$$2\,HAuCl_4 + 3\,(CH_3)_2NCOH + 3\,H_2O \rightarrow 2\,Au + 3\,(CH_3)_2NCOOH + 8\,H^+ + 8\,Cl^- \quad (1)$$

In this reaction, DMF serves as both the solvent and reducing agent. Water is essential for the oxidation of DMF, which can accelerate the reaction rate and thus cause the Au^{3+} ions to be more quickly reduced into atoms. At the

same time, it promotes the generation of protons and chloride ions. It is known that the presence of an oxidant (e.g., the oxygen from air) and a ligand (such as chloride) capable of coordinating to the metal ions in the reaction solution can result in a powerful etchant to oxidize zero-valent atoms back to the ionic form. This process is known as oxidative etching, and it has been observed in the solution-phase syntheses of various noble-metal nanocrystals including Ag, Au, Pd, Pt, and Rh.[33,37–42] In the present case, the oxygen/chloride pairs can etch away the corners of an octahedron, forming a highly truncated shape. Additionally, the presence of protons can also enhance the etching process and thus increase the degree of truncation.

We have tried to elucidate the function of PVP during the formation of Au octahedra. When a relatively low concentration of PVP was used (1/10 of the standard synthesis), much bigger octahedra, as well as truncated bipyramids and small, irregular nanocrystals, were obtained (see Figure 6A).

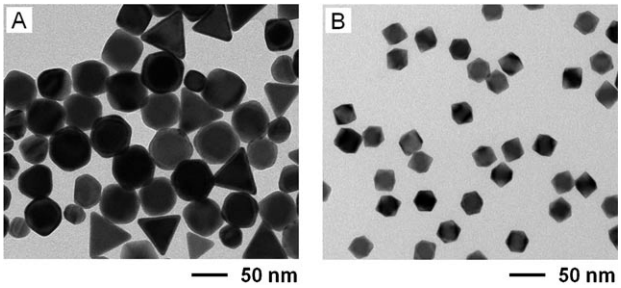

Figure 6. TEM images of Au nanocrystals prepared using the standard procedure except the use of PVP at two other different concentrations: A) 21.3 mM and B) 107 mM.

In this case, insufficient stabilization due to the relatively low concentration of PVP likely resulted in random aggregation for the seeds, and thus forming both single- and multiple-twinned nanocrystals. When the concentration of PVP was increased to a level of more than 100 mM, Au octahedra with a uniform size were obtained. Figure 6B shows TEM image of the Au octahedra that were prepared by using the standard procedure except the use of PVP at a lower concentration of 107 mM (half of the standard synthesis). The Au octahedra showed slightly sharper corners and edges as compared to those shown in Figure 1, and the edge length was also slightly increased to approximately 27 nm. This observation is consistent with the previous report that PVP can stabilize the {111} facets of Au nanocrystals when used at a relatively high concentration. When used at a relatively low concentration of, the PVP could not sufficiently stabilize the Au nanocrystals and thus leading to the formation of Au nanocrystals with poorly defined in shape and size.[43] We also compared the sizes and shapes of Au nanocrystals prepared at different reaction temperatures ranging from 60 °C to 140 °C. No significant change was observed in both size and shape for the resultant Au nanocrystals (see Figure S4 in the Supporting Information).

Conclusion

We have demonstrated the preparation of uniform Au octahedra in high purity by seeded growth. First, we obtained single-crystal seeds of Au spheres approximately 11 nm in diameter and with a percentage approaching 100% of the product. Uniform Au octahedra were then prepared by seeded growth with the Au spheres as seeds in DMF containing PVP and a relatively small amount of water. The edge lengths of resultant Au octahedra could be tightly controlled from 16 nm to 77 nm by simply varying the amount of Au seeds, the concentration of $HAuCl_4$, or both. The use of single-crystal seeds with a spherical shape and uniform distribution in size also enabled us to gain a better understanding of the effects of various reaction parameters on the shape evolution of nanocrystals.

Experimental Section

Chemicals: Gold(III) chloride trihydrate ($HAuCl_4 \cdot 3H_2O$, $\geq$ 99.0%), *N,N*-dimethylformamide (DMF, $\geq$ 99%), sodium borohydride ($NaBH_4$, 99%), L-ascorbic acid (AA, > 99%), poly(vinyl pyrrolidone) (PVP, Mw $\approx$55000), cetyltrimethylammonium bromide (CTAB, $\geq$ 99%), and cetyltrimethylammonium chloride (CTAC, $\geq$ 98%) were all obtained from Sigma–Aldrich and used as received. In all experiments, we used deionized water with a resistivity of 18 MΩ, which was prepared using an ultrapure water system (Aqua Solutions).

Synthesis of spherical Au seeds: The single-crystal spherical Au seeds were prepared using a two-step procedure.[34,35] We first prepared 3 nm Au nanoparticles by adding 10 mM ice-cold $NaBH_4$ aqueous solution (0.6 mL) to an aqueous solution containing 0.25 mM of $HAuCl_4$ and 0.1 M CTAB (10 mL), generating a brownish solution. The seed solution was kept undisturbed for 3 h at 27 °C to ensure complete decomposition of $NaBH_4$ remaining in the solution. Second, 0.5 mM $HAuCl_4$ (6 mL), 0.2 M CTAC (6 mL), and 0.1 M AA aqueous solutions (4.5 mL) were mixed in a glass vial, followed by the addition of the as-prepared suspension of 3 nm Au nanoparticles (0.3 mL). The final mixture turned from colorless into red within 1 min, indicating the formation of larger Au nanocrystals. After 1 h, a UV/Vis spectrum was recorded from the Au nanocrystal suspension, and the products were collected by centrifugation (14000 rpm, 30 min) and then washed with water once. The as-obtained Au spherical Au seeds were approximately 11 nm in diameter and they were re-dispersed in water. As determined by inductively-coupled plasma mass spectrometry (ICP-MS, ELAN DRC II, Perkin–Elmer) and TEM imaging, the concentration of Au in the seed suspension was found to be 54.6 mg L^{-1} (the corresponding Au nanoparticle concentration was 3.7×10^{15} particles per L).

Synthesis of Au octahedra: In a standard synthesis, DMF (5.8 mL) containing 0.162 mM of $HAuCl_4$ and 0.213 M of PVP was placed in a 20 mL glass vial, followed by the addition of a 11 nm spherical Au seed suspension (0.1 mL) and water (0.1 mL) at room temperature. The molar concentration of PVP was calculated in terms of the repeating unit. The vial was then capped and heated in an oil bath at 80 °C under magnetic stirring for 1 h. After that, the product was collected by centrifugation at 14000 rpm for 10 min, and then washed with water twice. The product was finally re-dispersed in ethanol for further characterization. To investigate the influence of water on the shape of Au nanocrystals, a certain amount of DMF was replaced by water while the total volume of the reaction mixture and concentration of the precursor were remained the same. To obtain Au octahedra with different sizes, the amount of Au seeds or the concentration of $HAuCl_4$ solution was varied.

Characterization: The SEM images were recorded with a field-emission microscope (Nova NanoSEM 230, FEI) operated at an accelerating volt-

age of 20 kV. The TEM images were recorded with an electron microscope (G2 Spirit Twin, FEI) operated at an accelerating voltage of 120 kV. The HRTEM images were recorded with a field-emission transmission electron microscope (JEM-2100F, JEOL) operated at an accelerating voltage of 200 kV. The samples were prepared by placing a few drops of the colloidal suspension in ethanol either on silicon substrates for SEM or on copper grids coated with carbon for TEM and HRTEM. The UV/Vis-NIR spectra were recorded with a UV/Vis-NIR spectrometer (Cary 50, Varian) with the particles suspended in ethanol. The concentration of Au was determined by ICP-MS and converted to the number of Au particles. The sample for ICP-MS was prepared by dissolving the Au particles in a mixture of hydrochloric acid (HCl, 37% in volume, 0.3 mL) and nitric acid (HNO_3, 70% in volume, 0.1 mL), followed by dilution with water until the HCl content reached 2% (volume) in the final solution.

Acknowledgements

This work was supported in part by the NSF (DMR-0804088) and startup funds from Washington University in St. Louis. As a visiting student from KAIST, D.Y.K. was also partially supported by the BK21 graduate program through the National Research Foundation of Korea funded by the Ministry of Education, Science and Technology. Part of the research was performed at the Nano Research Facility (NRF), a member of the National Nanotechnology Infrastructure Network (NNIN), which is supported by the NSF under award ECS-0335765.

[1] K. L. Kelly, E. Coronado, L. L. Zhao, G. Schatz, *J. Phys. Chem. B* **2003**, *107*, 668.
[2] E. E. Connor, J. Mwamuka, A. Gole, C. J. Murphy, M. D. Wyatt, *Small* **2005**, *1*, 325.
[3] L. Au, D. Zheng, F. Zhou, Z.-Y. Li, X. Li, Y. Xia, *ACS Nano* **2008**, *2*, 1645.
[4] M.-C. Daniel, D. Astruc, *Chem. Rev.* **2004**, *104*, 293.
[5] N. L. Rosi, C. A. Mirkin, *Chem. Rev.* **2005**, *105*, 1547.
[6] K. A. Willets, R. P. Van Duyne, *Ann. Rev. Phys. Chem.* **2007**, *58*, 267.
[7] J. Zhang, Y. Gao, R. A. Alvarez-Puebla, J. M. Buriak, H. Fenniri, *Adv. Mater.* **2006**, *18*, 3233.
[8] P. K. Jain, X. Huang, I. H. El-Sayed, M. A. El-Sayed, *Acc. Chem. Res.* **2008**, *41*, 1578.
[9] J. J. Storhoff, A. D. Lucas, V. Garimella, Y. P. Bao, U. R. Müller, *Nat. Biotechnol.* **2004**, *22*, 883.
[10] P. Fortina, L. J. Kricka, D. J. Graves, J. Park, T. Hyslop, F. Tam, N. Halas, S. Surrey, S. A. Waldman, *Trends Biotechnol.* **2007**, *25*, 145.
[11] C. Burda, X. Chen, R. Narayanan, M. A. El-Sayed, *Chem. Rev.* **2005**, *105*, 1025.
[12] A. R. Tao, S. Habas, P. Yang, *Small* **2008**, *4*, 310.
[13] Y. Xia, N. J. Halas, *Mater. Res. Soc. Bull.* **2005**, *30*, 338.
[14] F. Kim, S. Connor, H. Song, T. Kuykendall, P. Yang, *Angew. Chem.* **2004**, *116*, 3759; *Angew. Chem. Int. Ed.* **2004**, *43*, 3673.
[15] D. Seo, J. C. Park, and H. Song, *J. Am. Chem. Soc.* **2006**, *128*, 14863.
[16] N. R. Jana, L. Gearheart, C. J. Murphy, *Adv. Mater.* **2001**, *13*, 1389.
[17] Y.-Y. Yu, S.-S. Chang, C.-L. Lee, C. R. Chris Wang, *J. Phys. Chem. B* **1997**, *101*, 6661.
[18] F. Kim, J. H. Song, P. Yang, *J. Am. Chem. Soc.* **2002**, *124*, 14316.
[19] C. Cao, S. Park, S. J. Sim, *J. Colloid Interface Sci.* **2008**, *322*, 152.
[20] T. H. Ha, H.-J. Koo, B. H. Chung, *J. Phys. Chem. C* **2007**, *111*, 1123.
[21] C. J. Murphy, T. K. Sau, A. M. Gole, C. J. Orendorff, J. Gao, L. Gou, S. E. Hunyadi, T. Li, *J. Phys. Chem. B* **2005**, *109*, 13857.
[22] H. Reiss, *J. Chem. Phys.* **1951**, *19*, 482.
[23] X. Peng, J. Wickham, A. P. Alivisatos, *J. Am. Chem. Soc.* **1998**, *120*, 5343.
[24] Y. Ma, J. Zeng, W. Li, M. McKiernan, Z. Xie, Y. Xia, *Adv. Mater.* **2010**, *22*, 1930.
[25] P. Qiu, C. Mao, *J. Nanopart. Res.* **2008**, *11*, 885.
[26] C. Li, K. L. Shuford, Q.-H. Park, W. Cai, Y. Li, E. J. Lee, S. O. Cho, *Angew. Chem.* **2007**, *119*, 3328; *Angew. Chem. Int. Ed.* **2007**, *46*, 3264.
[27] C. Li, K. L. Shuford, M. Chen, E. J. Lee, S. O. Cho, *ACS Nano* **2008**, *2*, 1760.
[28] C.-C. Chang, H.-L. Wu, C.-H. Kuo, M. Huang, *Chem. Mater.* **2008**, *20*, 7570.
[29] W. Niu, S. Zheng, D. Wang, X. Liu, H. Li, S. Han, J. Chen, Z. Tang, G. Xu, *J. Am. Chem. Soc.* **2009**, *131*, 697.
[30] Y. Huang, W. Wang, H. Liang, H. Xu, *Cryst. Growth Des.* **2009**, *9*, 858.
[31] D. Kim, J. Heo, M. Kim, Y. W. Lee, S. W. Han, *Chem. Phys. Lett.* **2009**, *468*, 245.
[32] J. Zhang, H. Liu, Z. Wang, N. Ming, *Appl. Phys. Lett.* **2007**, *90*, 163122.
[33] W. Li, Y. Xia, *Chem. Asian J.* **2010**, *5*, 1312.
[34] F.-R. Fan, D.-Y. Liu, Y.-F. Wu, S. Duan, Z.-X. Xie, Z.-Y. Jiang, Z.-Q. Tian, *J. Am. Chem. Soc.* **2008**, *130*, 6949.
[35] Y. Ma, W. Li, E. C. Cho, Z. Li, T. Yu, J. Zeng, Z. Xie, Y. Xia, *ACS Nano* **2010**, *4*, 6725.
[36] I. Pastoriza-Santos, L. M. Liz-Marzán, *Adv. Funct. Mater.* **2009**, *19*, 679.
[37] S. H. Im, Y. T. Lee, B. Wiley, Y. Xia, *Angew. Chem.* **2005**, *117*, 2192; *Angew. Chem. Int. Ed.* **2005**, *44*, 2154.
[38] B. J. Wiley, T. Herricks, Y. Sun, Y. Xia, *Nano Lett.* **2004**, *4*, 1733.
[39] B. J. Wiley, Y. Xiong, Z.-Y. Li, Y. Yin, Y. Xia, *Nano Lett.* **2006**, *6*, 765.
[40] Y. Xiong, H. Cai, B. J. Wiley, J. Wang, M. J. Kim, Y. Xia, *J. Am. Chem. Soc.* **2007**, *129*, 3665.
[41] Y. Xiong, J. M. McLellan, J. Chen, Y. Yin, Z.-Y. Li, Y. Xia, *J. Am. Chem. Soc.* **2005**, *127*, 17118.
[42] N. Zettsu, J. M. McLellan, B. Wiley, Y. Yin, Z.-Y. Li, Y. Xia, *Angew. Chem.* **2006**, *118*, 1310; *Angew. Chem. Int. Ed.* **2006**, *45*, 1288.
[43] D. Y. Kim, S. H. Im, O. O. Park, Y. T. Lim, *CrystEngComm* **2010**, *12*, 116.

Received: February 1, 2011
Published online: March 17, 2011

